



Published in final edited form as:

J Thorac Cardiovasc Surg. 2017 September ; 154(3): 955–963. doi:10.1016/j.jtcvs.2017.04.081.

Layered Smooth Muscle Cell-Endothelial Progenitor Cell Sheets Derived From the Bone Marrow Augment Post-Infarction Ventricular Function

Yasuhiro Shudo, MD, PhD¹, Andrew B. Goldstone, MD¹, Jeffrey E. Cohen, MD¹, Jay B. Patel, BS¹, Michael S. Hopkins, BS¹, Amanda N. Steele, BS¹, Bryan B. Edwards, BE¹, Masashi Kawamura, MD, PhD¹, Shigeru Miyagawa, MD, PhD², Yoshiki Sawa, MD, PhD², and Y. Joseph Woo, MD¹

¹Department of Cardiothoracic Surgery, Stanford University School of Medicine

²Department of Cardiovascular Surgery, Osaka University Graduate School of Medicine

Abstract

Objective—The angiogenic potential of endothelial progenitor cells (EPCs) may be limited by the absence of their natural biologic foundation, namely smooth muscle pericytes. We hypothesized that joint delivery of EPCs and smooth muscle cells (SMCs) in a novel, totally bone marrow-derived cell sheet will mimic the native architecture of a mature blood vessel and act as an angiogenic construct to limit post infarction ventricular remodeling.

Methods—Primary EPCs and mesenchymal stem cells (MSCs) were isolated from bone marrow of Wistar rats. MSCs were transdifferentiated into SMCs by culture on fibronectin-coated culture dishes. Confluent SMCs topped with confluent EPCs were detached from an Upcell dish to create a SMC-EPC bi-level cell sheet. A rodent model of ischemic cardiomyopathy was then created by ligating the left anterior descending artery. Rats were randomized into three groups: cell sheet transplantation (n=9), no treatment (n=12), or sham surgery control (n=7).

Results—Four weeks post infarction mature vessel density tended to increase in cell sheet-treated animals compared with controls. Cell sheet therapy significantly attenuated the extent of cardiac fibrosis compared with that of the untreated group (untreated vs. cell sheet, 198 degrees (IQR, 151 degrees – 246 degrees) vs. 103 degrees (IQR, 92 degrees – 113 degrees), p=0.04). Furthermore, EPC-SMC cell sheet transplantation attenuated myocardial dysfunction, as evidenced by an increase in LV ejection fraction (untreated vs. cell sheet vs sham, 33.5% (IQR, 27.8%–35.7%) vs. 45.9% (IQR, 43.6%–48.4%) vs. 59.3% (IQR, 58.8%–63.5%), p=0.001) and decreases in LV dimensions.

Address for Correspondence: Y. Joseph Woo, MD, Department of Cardiothoracic Surgery, Falk Cardiovascular Research Center, Stanford University School of Medicine, Stanford, CA 94305. joswoo@stanford.edu.

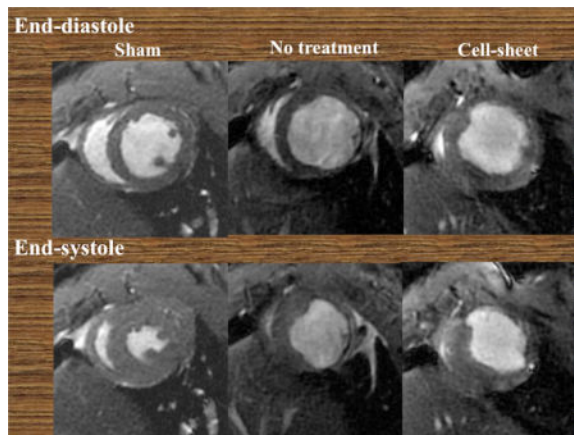
Publisher's Disclaimer: This is a PDF file of an unedited manuscript that has been accepted for publication. As a service to our customers we are providing this early version of the manuscript. The manuscript will undergo copyediting, typesetting, and review of the resulting proof before it is published in its final citable form. Please note that during the production process errors may be discovered which could affect the content, and all legal disclaimers that apply to the journal pertain.

Conflicts of Interest: None

The data in this manuscript was presented at the American Association for Thoracic Surgery's 96th Annual Meeting, Baltimore, MD

Conclusions—The bone marrow-derived, spatially arranged SMC-EPC bi-level cell sheet is a novel, multi-lineage cellular therapy obtained from a translationally practical source. Interactions between SMCs and EPCs augment mature neovascularization, limit adverse remodeling, and improve ventricular function after myocardial infarction.

Graphical abstract



INTRODUCTION

Despite medical and surgical advances, heart disease is the leading cause of death in the United States. Better characterization of stem cell lineages and endogenous effectors of myocardial repair has burgeoned interest in employing cell therapies to improve left ventricular (LV) function in patients with advanced heart disease.

Tissue engineering is an essential component of developing effective regenerative therapies.⁵ In the past decade, tissue engineered cell and scaffold therapies have been widely investigated, and several products are now commercially available. Scaffold-based tissue engineering is particularly popular, and includes technologies such as biodegradable scaffolds,⁶ decellularized tissues,⁷ hydrogel and cell mixtures,⁸ bioprinting,⁹ and fiber-based tissue engineering.¹⁰ However, our group employs scaffold-free technology for cell sheet engineering.¹¹ The cell sheet is created on, and removed from a specialized dish that is covalently grafted with a temperature-responsive polymer – poly (N-isopropylacrylamide) – which undergoes an enzyme-free transformation from hydrophobic to hydrophilic by simply lowering the temperature.¹² Thus, the specialized dishes permit fabrication of three-dimensional tissues from densely adherent cells, without an artificial scaffold or enzymatic digestion. Cell sheets are easily manipulated and have a unique ability to integrate within native tissue; they retain cell-cell junctions as well as the extracellular matrix (ECM) deposited on the basal surface of cell sheet.⁴

We previously demonstrated that engineered cell sheets with smooth muscle cells (SMC) and endothelial progenitor cells (EPC) harnessed natural interactions between EPCs and SMCs, created structurally mature, functional microvasculature, and induced functional recovery of distressed myocardium.¹ However, cell sheet SMCs were obtained from the thoracic aorta, and therefore precluded clinical translation.¹ To resolve this problem, we

have noted that bone marrow-derived mesenchymal stem cells (MSC) have shown potential to differentiate into various cell types, including SMCs.² Given that the ECM is a powerful regulator of SMC phenotypic modulation,³ we demonstrated that fibronectin helped guide differentiation of MSCs into SMCs, while simultaneously preserving cellular proliferative capacity.⁴

In this study, we hypothesized that joint delivery of EPCs and SMCs in a novel, totally bone marrow derived cell sheet will mimic the native architecture of a mature blood vessel and act as a suprathereapeutic angiogenic construct to limit post infarction ventricular remodeling.

MATERIALS AND METHODS

Isolation of MSCs and EPCs

Bone marrow mononuclear cells were isolated from the long bones of male Wistar rats (8 weeks old, 250–300g; Charles River), filtered through a 40 μ m cell strainer (Falcon), and centrifuged at 300G for 7 minutes. Red blood cells were excluded using 1 \times RBC lysis buffer (eBioscience, #00-4337-57) for 10 minutes at 4°C. Remaining cells were cultured in a medium with Dulbecco's Modified Eagle's Medium (DMEM) (Gibco, #11995-040) containing 10% fetal bovine serum (FBS) (Sigma-Aldrich) and gentamicin on non-coated culture dishes for 24 hours at 37°C. Following incubation, the adherent cells were washed and then cultured in a medium with DMEM containing 10% FBS and gentamicin. A purified population of MSCs was obtained 10 to 14 days after the initiation of culture. MSCs were identified in accordance with the criteria of the International Society for Cellular Therapy;² specifically, expression of CD 105, CD73, and CD 90, as well as absent expression of CD45 and CD34 were required.⁴

EPCs were isolated and cultured as previously described.¹ Briefly, bone marrow mononuclear cells were isolated from the long bones of Wistar rats by density gradient centrifugation with Histopaque 1083 (Sigma-Aldrich) and cultured in endothelial basal medium-2 supplemented with EGM-2 SingleQuot (Lonza) containing human epidermal growth factor, 5% FBS, vascular endothelial growth factor (VEGF), basic human fibroblast growth factor, recombinant human long R3 insulin-like growth factor-1, ascorbic acid, and gentamicin on vitronectin (Sigma-Aldrich, V0132-50VG) coated dishes. The combination of endothelium-specific media and the removal of non-adherent bone marrow mononuclear cells were intended to select for the EPC phenotype. The EPC phenotype was confirmed by expression of CD 31, as previously described.⁴

Transdifferentiation of MSCs into SMCs

Primary rodent MSCs were transferred and cultured in a medium with DMEM and 10% FBS on 60mm culture dishes coated with fibronectin (FN group, BD Biosciences) at 37 °C in a humidified atmosphere of 5% CO₂ in air. Primary MSCs were also included in this study (Control group). The cell number of the primary seeded MSCs was 4–6 \times 10³/cm² for each plate. MSC growth medium was used as the nutrient medium and all media were exchanged every 48–72 hours.⁴

Nanovolume Capillary Electrophoresis-Based Protein Analysis of Cultured Cells

Nanovolume capillary electrophoresis-based protein analysis was performed on the cultured MSCs, and SMCs with Wes™ (ProteinSimple Inc., San Jose, CA). Tissue homogenates from cultured cells were prepared using Halt™ Protease Inhibitor Single-Use Cocktail (ThermoScientific) diluted in T-PER Tissue Protein Extraction Reagent (ThermoScientific). The protein concentration for the lysate was estimated by Bio-Rad Protein Assay Dye Reagent Concentrate (Bio-Rad Laboratories, Inc.).

For each analysis, we applied as little as 2 pg of protein to the pre-filled plate according to the manufacturer's instructions. A charge-based separation (isoelectric focusing) was performed in a 5 cm-long, 100 µm-inner diameter capillary cartridge. After separation and within-capillary immobilization, specific antibodies were applied to detect proteins of interest. Antibodies included rabbit polyclonal anti-alpha smooth muscle actin antibody (Abcam, ab5694, 1:50), rabbit polyclonal anti-SM22 alpha antibody (Abcam, ab14106, 1:50), rabbit monoclonal anti-caldesmon antibody (Abcam, ab32330, 1:50), or vinculin (Abcam, ab129002, 1:500). To assess the intensity of bands for these proteins semi-quantitatively, densitometric analysis was performed using Compass software. The intensity level of detected protein bands was dividing by the intensity level of vinculin for standardization.

Creation of Bi-level Cell Sheet

SMCs were plated at a density of $1.5 \times 10^5/\text{cm}^2$ in a 35mm Upcell dish – which is grafted with temperature-responsive polymers (CellSeed, Tokyo, Japan) – and then cultured in EPC-specific medium. After 24 hours of culture at 37°C and 5% CO₂, EPCs were added at an equivalent density of $1.5 \times 10^5/\text{cm}^2$ onto the Upcell dish, which was already confluent with SMCs. Each dish was transferred to room temperature for 30 minutes following an additional 24 hours in culture; a confluent bi-level cell sheet, made of EPCs and transdifferentiated SMCs, was then spontaneously detached as an intact cell sheet from the UpCell dish.

Immunohistological Assessment of Bi-level Cell Sheet

The cell sheet, which consisted of EPCs and SMCs transdifferentiated from MSCs, was embedded in an optimum cutting temperature compound for 10 µm-thick sections. Cryosections were stained with rabbit polyclonal anti-alpha smooth muscle actin antibody (Abcam, ab5694, 1:100) and mouse monoclonal anti-CD31 antibody (Abcam ab64543, 1:00) to assess characteristics of bi-level cell sheet.

Rat Model of Ischemic Cardiomyopathy and Cell Sheet Transplantation

Female Wistar rats (8 weeks old, 250–300g; Charles River) were anesthetized with isoflurane, endotracheally intubated with a 19-gauge catheter, and mechanically ventilated (Hallowell EMC). Anesthesia was maintained by inhalation of 2.0% isoflurane. The proximal left anterior descending coronary artery (LAD) of Wistar rats was permanently occluded using a left thoracotomy approach. This produced a consistent and reproducible myocardial infarction encompassing 35% to 40% of the left ventricle.¹ Within 5 minutes after LAD ligation, each rat was allocated into one of two groups by simple randomization:

those that underwent co-cultured cell sheet transplantation (cell sheet group, n=9), and those that underwent no treatment (untreated control group, n=12). For comparative purposes, rats receiving a sham operation were also studied as a positive control (sham surgery control group, n=7). In the cell sheet group, the co-cultured bi-level cell sheet, which consisted of $1.5 \times 10^5/\text{cm}^2$ EPCs and $1.5 \times 10^5/\text{cm}^2$ SMCs, was placed on the epicardium covering the ischemic area. Animals were then kept in temperature-controlled individual cages for 4 weeks. The rats were euthanized 4 weeks after surgery by intravenous injection of 2mEq/kg potassium chloride solution under terminal anesthesia, and the heart was excised.

MRI Assessment of Cardiac Function

ECG-gated cardiac magnetic resonance imaging (MRI) was performed using a preclinical 7T (MR901 Discovery) horizontal bore scanner (Agilent, Santa Clara, CA) with a shielded gradient system (600mT/m) 1–3 days before, and 4 weeks after myocardial infarction (cell sheet, n=9; no treatment, n=12; sham surgery, n=7). Animals were anesthetized with 3.0% inhaled isoflurane, and placed onto an animal cradle in prone position. Animals were kept at $37 \pm 0.4^\circ\text{C}$ (during image acquisition) via an air heating system while oxygen and anesthetics (1–2% isoflurane) were supplied via a nose cone (0.5L/min). Data acquisition was performed with a 4-channel phased array receive only surface coil (Rapid MR International, Columbus, OH) placed around the heart and centered in a decoupled 72mm transmit/receive volume coil (Agilent). Long- and short-axis scout images were acquired to define the two- and four-chamber long-axis views. The cine long-axis views were used to define the short-axis orientation. A prospectively double gated (ECG and respiration) spoiled gradient echo sequence was used to acquire cine cardiac images with the following parameters for standard cine acquisitions: TE 1.5ms, TR 6–8ms, flip angle 15° , slice thickness 1mm, no slice separation, FOV $50 \times 50\text{mm}^2$, matrix size 192×192 , NSA 1 for short-axis and 2 for long-axis. Twenty cine frames were recorded to cover the cardiac cycle. A single short-axis slice was obtained in approximately 45 seconds, leading to a total scan time of 11–13 min covering the heart from base to apex (14–15 slices).

Imaging parameters for these acquisitions were as follows: TE 1.4 ms, TR one breathing interval, TI 280–370ms, flip angle 90° , slice thickness 1mm, no slice separation, FOV $40 \times 40\text{mm}^2$, matrix size 192×192 , NSA 2, views per segment 2. The acquisition time was roughly 1 minute per slice. The imaging protocol for one rat typically required 45–50 minutes. All images from one animal were combined into a dataset, randomized, and anonymized. Data analysis was performed using the semi-automatic segmentation software Segment (Medviso AB, Sweden) as previously described.¹³

Routine parameters of LV geometry and function – such as LV end-diastolic volume (LVEDV), end-systolic volume (LVESV), and LV ejection fraction (LVEF) – were measured according to the slice summation method using LV functional analysis software (Osiri× MD Imaging Software, version 3.0). All analyses were performed by a single investigator in a group-blinded fashion.

Assessment of Mature Vessel Formation

Four weeks post myocardial infarction, all rat hearts were dissected and embedded in an optimum cutting temperature compound for 10 μm -thick sections. Heart cryosections were stained with sheep polyclonal anti-von Willebrand factor (vWF) antibody (Abcam, ab8822, 1:100) and rabbit polyclonal anti-alpha smooth muscle actin (SMA) antibody (Abcam, ab5694, 1:100) to assess mature vessel density. Mature vessel density was calculated as the number of positively stained vessels in five randomly selected fields within the peri-infarct border zone, per heart. Cell nuclei were counterstained with 6-diamidino (DAPI, Vector Laboratories). Images were acquired with fluorescence microscopy (Leica) and ImageJ software was used for quantitative morphometric analyses.

Assessment of Myocardial Fibrosis

Four weeks after the treatment, the hearts were explanted, embedded in optimum cutting temperature compound, and cut into 10 μm thick sections. Massons trichrome staining was performed to assess cardiac fibrotic extension. The fibrotic burden was calculated as the degree of fibrosis along the circumferential length of the LV at the mid-LV level, which was defined as the mid-point between the base and apex of the LV (n=4 per group).

Statistical Analysis

Continuous variables are expressed as the median and interquartile range (IQR). Due to small sample sizes, comparisons between two groups were made using the Wilcoxon-Mann-Whitney *U* test. For comparisons between three groups, we used the Kruskal-Wallis test followed by post hoc pairwise Wilcoxon-Mann-Whitney *U* tests. The multiplicity in pairwise comparisons was corrected by the Bonferroni procedure. For categorical variables, two groups were compared using Fisher's exact test. A p-value less than 0.05 was considered statistically significant. All calculations were performed using JMP 9.0 (SAS Institute Inc, Cary, NC).

Animal Care and Biosafety

Wistar rats were obtained from Charles River. Food and water were provided ad libitum. This investigation conformed with the *Guide for the Care and Use of Laboratory Animals* published by the US National Institutes of Health (NIH Publication No. 85-23, revised 1996) and was approved by the Institutional Animal Care and Use Committee of Stanford University (protocol 28921).

RESULTS

Characterization of MSCs and Transdifferentiated SMCs with ECM

Proportions of proteins indicative of the SMC phenotype were examined by nanovolume capillary electrophoresis-based protein analysis. MSCs were isolated from bone marrow and transdifferentiated via culture on fibronectin-coated dishes. Expression levels of alpha SMA (MSC vs. SMC, 0.11 (IQR, 0.10–0.13) vs. 0.62 (IQR, 0.54–0.67), $p=0.04$), SM22 (MSC vs. SMC, 0.010 (IQR, 0.010–0.013) vs. 0.490 (IQR, 0.419–0.570), $p=0.04$), and caldesmon (MSC vs. SMC, 0.005 (IQR, 0.005–0.007) vs. 0.413 (IQR, 0.315–0.524), $p=0.04$) were

significantly elevated in transdifferentiated MSCs compared to that of primary MSCs (Figure 1).

Characterization of Bi-level Cell Sheet

The bi-level cell sheet maintained alpha SMA positive SMCs and CD31 positive EPCs in separate layers in vitro (Figure 2A).

Co-administered EPCs and SMCs Likely Enhance Intramyocardial Arterial Density

Four weeks post myocardial infarction, a larger number of arteries (vWF/alpha SMA-positive blood vessels) were detected in the cell sheet-treated myocardium compared with that of the untreated group (untreated vs. cell sheet, $18/\text{mm}^2$ (IQR, $16/\text{mm}^2$ – $29/\text{mm}^2$) vs. $37/\text{mm}^2$ ($25/\text{mm}^2$ – $120/\text{mm}^2$), $p=0.08$), but this result only approached our threshold for statistical significance (Figure 2B, C).

EPC-SMC Cell Sheet Attenuates Cardiac Fibrosis

In the untreated group, abundant fibrotic changes were observed in the infarct area, whereas fibrotic change was attenuated in the cell sheet-treated group, as shown by Masson's trichrome staining.

Four weeks after myocardial infarction, cell sheet therapy significantly attenuated the extent of cardiac fibrosis compared with that of the untreated group, as demonstrated by Masson's trichrome staining (untreated vs. cell sheet, 198 degrees (IQR, 151 degrees – 246 degrees) vs. 103 degrees (IQR, 92 degrees – 113 degrees), $p=0.04$) (Figure 3); no fibrosis was noted in the sham group.

EPC-SMC Cell Sheet Improves Cardiac Function and Attenuates Left Ventricular Remodeling

The effects of co-cultured bi-level cell sheet transplantation on cardiac function were assessed in a rat model of ischemic cardiomyopathy. Compared to sham surgery, permanent ligation of the LAD in untreated animals significantly decreased LV ejection fraction with concomitant increases in LV end systolic and end diastolic volume four weeks after infarction, which are all characteristics of chronic ischemic heart failure. However, EPC-SMC cell sheet transplantation attenuated myocardial dysfunction, as evidenced by an increase in LV ejection fraction (untreated vs. cell sheet vs sham, 33.5% (IQR, 27.8%–35.7%) vs. 45.9% (IQR, 43.6%–48.4%) vs. 59.3% (IQR, 58.8%–63.5%), $p=0.001$) and induced significant reverse LV remodeling, as evidenced by decreases in LV dimensions (LVEDV, untreated vs. cell sheet vs. sham, $688\mu\text{l}$ (IQR, $604\mu\text{l}$ – $787\mu\text{l}$) vs. $586\mu\text{l}$ (IQR, $505\mu\text{l}$ – $661\mu\text{l}$) vs. $416\mu\text{l}$ (IQR, $399\mu\text{l}$ – $469\mu\text{l}$), $p=0.001$; LVESV, untreated vs. cell sheet vs. sham, $446\mu\text{l}$ (IQR, $374\mu\text{l}$ – $557\mu\text{l}$) vs. $317\mu\text{l}$ (IQR, $266\mu\text{l}$ – $372\mu\text{l}$) vs. $151\mu\text{l}$ (IQR, $147\mu\text{l}$ – $191\mu\text{l}$), $p=0.001$) (Figure 4).

DISCUSSION

Development of novel therapies that are clinically translatable is critical if one hopes to transition research from the bench to the bedside. Although our prior EPC-SMC cell sheets

were potent angiogenic constructs, using the aorta as a source for SMC isolation precluded translation as a realistic therapy. Here, we demonstrate that MSCs may be encouraged toward the SMC phenotype simply by culturing bone marrow-derived MSCs on fibronectin-coated dishes. Then, a confluent co-cultured bi-level cell sheet made of isolated EPCs and transdifferentiated SMCs was engineered using cell sheet technology. The result: increased arterial density, as well as attenuated post infarction myocardial dysfunction and remodeling.

We have reported that bi-level cell sheets, consisting of co-cultured SMCs and EPCs, create architecturally mature, functional microvasculature by maintaining the natural interactions between EPCs and SMCs, thereby enhancing myocardial function beyond that of cell injection therapy.¹ Cell sheets deliver cells more effectively than intracoronary or intramyocardial injection because cell dispersion and myocardial injury are lessened. However, the ability to acquire the requisite cells in a less invasive and efficient fashion is crucial. To address this, the use of somatic adult stem cells (e.g. MSCs) has been suggested for use in regenerative medicine.¹⁵ MSCs are an attractive autologous cell source for cell-based regenerative therapies due to their strong ability to proliferate and differentiate into various cell types, including chondrocytes, osteocytes, adipocytes, skeletal myoblasts, and cardiomyocytes.^{16, 17} Moreover, MSCs can be isolated in a minimally invasive fashion from various tissues, such as the bone marrow, umbilical cord, amniotic fluid, peripheral blood, and adipose tissue. These concepts led us to examine MSCs as a potential source of SMCs for cell sheet engineering. By testing different types of ECM, we found that isolated MSCs can be reliably transdifferentiated into the SMC lineage – while simultaneously maintaining proliferative capacity – simply by culturing on commercially available fibronectin-coated dishes.⁴ Here, we provide evidence that the SMCs transdifferentiated from MSCs maintain their *in vivo* therapeutic capacity, an essential finding if such a therapy is to be translated to the clinical arena.

Tissue engineering therapeutics created from cells and scaffolds have been widely investigated. Cell sheet technology has been employed to regenerate a number of damaged tissues. Several studies, including clinical trials, have been conducted to examine whether cell sheets effectively repair the cornea, epithelium,¹⁸ or heart.^{11, 19} Confluent cells on a temperature responsive culture surface can be harvested as an intact and contiguous cell sheet by simply reducing the temperature without protease treatment. The significant features of the cell sheet are that cell-cell junctions and ECM components mediating cell adhesion are retained in the cell sheet without artificial scaffolds. In contrast, conventional cell harvesting using enzymatic digestion (e.g. trypsin) disrupts all cell-cell junctions and adhesive proteins between cells. The EPC-SMC bi-level cell sheet retained regional morphologic differences between different cell types following mobilization from the UpCell dish. As determined by scanning electron microscopy, the SMC layer contained spherical cells and the EPC layer formed a thin film-like monolayer.⁴

The mechanism by which the bone marrow derived EPC-SMC bi-level cell sheet limited adverse ventricular remodeling and improved cardiac function is complex. Its contribution to the creation of mature arteries seems to be essential; we have previously demonstrated with cell fate tracking that a bi-level cell sheet, which contained EPCs and SMCs in separate layers, directly incorporates into perfused vasculature and remains present 4 weeks post

infarction.¹ In the present study, cell sheet transplantation increased arterial density. One possible explanation is that maintenance of the interactions between EPCs and their physiologic support cell, SMCs, augments arterialization and in turn limits adverse remodeling after myocardial infarction.

For more than a decade, echocardiography has been used ubiquitously to measure LV function and volume in rodents with ischemic cardiomyopathy. However, results are based on geometric assumptions that limit data accuracy. Furthermore, assumptions within the calculations of parameters of cardiac function are typically violated after a myocardial infarction. Recent advances in cardiac MRI have resulted in a shorter acquisition time and improved image quality. As such, cardiac MRI is now considered the reference standard for accurate assessment of LV geometry and volume in humans. Cardiac MRI has also been used to evaluate cardiac function in small animals.¹³ It provides excellent temporal and spatial resolution, it is very accurate, and it facilitates reproducible quantitative measurements of cardiac structure and function.²⁰ In our study, cardiac MRI illustrated post infarction, eccentric adverse ventricular remodeling in both cell sheet-treated and untreated negative control groups. However, EPC-SMC cell sheet transplantation significantly enhanced ventricular function and attenuated ventricular remodeling compared with that of untreated controls. Because we employed an acute MI model in our study and only imaged the heart at a single time point, we cannot determine whether the observed changes in cardiac function and LV dimensions post-infarct were the result of reverse remodeling or simply mitigation of adverse remodeling.

Considering the time required to isolate, cultivate, transdifferentiate, and manipulate cells *in vitro*, this treatment strategy for acute myocardial infarction is not yet directly applicable to the clinical arena. However, such a construct may be a potential candidate for allogeneic therapy. Further investigation into the utility of these cell sheets in treating chronic ischemic cardiomyopathy and diabetic cardiomyopathy are ongoing, as is an assessment of the duration of transplanted cell survival. Finally, whether bi-layer cell sheets are incrementally more effective than EPC, SMC, or MSC monolayer cell sheets requires further testing.

In conclusion, the bone marrow derived, anatomically oriented bi-level cell sheet made of isolated EPCs and transdifferentiated SMCs is a novel, multi-lineage cellular therapy obtained from a translationally practical source. Delivery of a tissue engineered construct that maintains important interactions between EPCs and SMCs enhances mature neovascularization within border zone myocardium, tempers post infarction adverse remodeling, and strengthens ventricular function.

Acknowledgments

Funding: This study was supported by the National Institutes of Health (NIH) Grant 1R01HL089315-01 (Y.J.W); American Heart Association Great Rivers Affiliate Postdoctoral Fellowship co-sponsored by the Claude R. Joyner Fund for Young Medical Researchers (#12POST12060567) (Y.S.); Uehara Memorial Foundation for Research Fellow, Japan (Y.S.).

ABBREVIATIONS and ACRONYMS

LV left ventricular

ECM	extracellular matrix
SMC	smooth muscle cells
EPC	endothelial progenitor cells
MSC	mesenchymal stem cells
DMEM	Dulbecco's Modified Eagle's Medium
FBS	fetal bovine serum
VEGF	vascular endothelial growth factor
FN	fibronectin
LAD	left anterior descending coronary artery
MRI	magnetic resonance imaging
EDV	end-diastolic volume
ESV	end-systolic volume
EF	ejection fraction
vWF	von Willebrand factor
SMA	smooth muscle actin
GAPDH	glyceraldehyde 3-phosphate dehydrogenase

References

1. Shudo Y, Cohen JE, MacArthur JW, Atluri P, Hsiao PF, Yang EC, et al. Spatially oriented, temporally sequential smooth muscle cell-endothelial progenitor cell bi-level cell sheet neovascularizes ischemic myocardium. *Circulation*. 2013; 128(11 Suppl 1):S59–S68. [PubMed: 24030422]
2. Dominici M, Le Blanc K, Mueller I, Slaper-Cortenbach I, Marini F, Krause D, et al. Minimal criteria for defining multipotent mesenchymal stromal cells. The International Society for Cellular Therapy position statement. *Cytotherapy*. 2006; 8:315–317. [PubMed: 16923606]
3. Thyberg J, Hedin U, Sjolund M, Palmberg L, Bottger BA. Regulation of differentiated properties and proliferation of arterial smooth muscle cells. *Arteriosclerosis*. 1990; 10:966–990. [PubMed: 2244864]
4. Shudo Y, Cohen JE, Goldstone AB, MacArthur JW, Patel J, Edwards BB, et al. Transdifferentiation of Mesenchymal Stem Cell into Smooth Muscle Cell Lineage; Utility for Clinical Application From Isolation to Creation of Cell-Sheet. *Cytotherapy*. 2016; 18:510–517. [PubMed: 26971679]
5. Langer R, Vacanti JP. Tissue engineering. *Science*. 1993; 260:920–926. [PubMed: 8493529]
6. Atluri P, Trubelja A, Fairman AS, Hsiao PF, MacArthur JW, Cohen JE, et al. Normalization of Post-Infarct Biomechanics Utilizing a Novel Tissue Engineered Angiogenic Construct. *Circulation*. 2013 Sep 10; 128(26 Suppl 1):S95–104. [PubMed: 24030426]
7. Neumann A, Sarikouch S, Breyman T, Cebotari S, Boethig D, Horke A, et al. Early systemic cellular immune response in children and young adults receiving decellularized fresh allografts for pulmonary valve replacement. *Tissue Eng Part A*. 2014; 20:1003–1011. [PubMed: 24138470]

8. Cohen JE, Purcell BP, MacArthur JW Jr, Mu A, Shudo Y, Patel JB, et al. A bioengineered hydrogel system enables targeted and sustained intramyocardial delivery of neuregulin, activating the cardiomyocyte cell cycle and enhancing ventricular function in a murine model of ischemic cardiomyopathy. *Circ Heart Fail*. 2014; 7:619–626. [PubMed: 24902740]
9. Murphy SV, Atala A. 3D bioprinting of tissues and organs. *Nat Biotechnol*. 2014; 32:773–785. [PubMed: 25093879]
10. Onoe H, Okitsu T, Itoh A, Kato-Negishi M, Gojo R, Kiriya D, et al. Metre-long cell-laden microfibers exhibit tissue morphologies and functions. *Nat Mater*. 2013; 12:584–590. [PubMed: 23542870]
11. Sawa Y, Miyagawa S, Sakaguchi T, Fujita T, Matsuyama A, Saito A, et al. Tissue engineered myoblast sheets improved cardiac function sufficiently to discontinue LVAS in a patient with DCM: report of a case. *Surg Today*. 2012; 42:181–184. [PubMed: 22200756]
12. Okano T, Yamada N, Sakai H, Sakurai Y. A novel recovery system for cultured cells using plasma-treated polystyrene dishes grafted with poly (N-iso-propylacrylamide). *J Biomed Mater Res*. 1993; 27:1243–1251. [PubMed: 8245039]
13. Riegler J, Gillich A, Shen Q, Gold JD, Wu JC. Cardiac tissue slice transplantation as a model to assess tissue-engineered graft thickness, survival, and function. *Circulation*. 2014; 130(11 Suppl 1):S77–S86. [PubMed: 25200059]
14. Merk DR, Chin JT, Dake BA, Maeqdefessel L, Miller MO, Kimura N, et al. miR-29b participates in early aneurysm development in Marfan syndrome. *Circ Res*. 2012; 110:312–324. [PubMed: 22116819]
15. Shudo Y, Miyagawa S, Ohkura H, Fukushima S, Saito A, Shiozaki M, et al. Addition of mesenchymal stem cells enhances the therapeutic effects of skeletal myoblast cell-sheet transplantation in a rat ischemic cardiomyopathy model. *Tissue Engineering Part A*. 2013; 20:728–739.
16. Jiang Y, Jahagirdar BN, Reinhardt RL, Schwartz RE, Keene CD, Ortiz-Gonzalez XR, et al. Pluripotency of mesenchymal stem cells derived from adult marrow. *Nature*. 2002; 418:41–49. [PubMed: 12077603]
17. Prockop DJ. Marrow stromal cells as stem cells for non-hematopoietic tissues. *Science*. 1997; 276:71–74. [PubMed: 9082988]
18. Nishida K, Yamato M, Hayashida Y, Watanabe K, Yamamoto K, Adachi E, et al. Corneal reconstructin with tissue-engineered cell sheets composed of autologous oral mucosal epithelium. *N Engl J Med*. 2004; 351:1187–1196. [PubMed: 15371576]
19. Shudo Y, Miyagawa S, Fukushima S, Saito A, Shimizu T, Okano T, et al. Novel regenerative therapy using cell-sheet covered with omentum flap delivers a huge number of cells in a porcine myocardial infarction model. *J Thorac Cardiovasc Surg*. 2011; 142:1188–1196. [PubMed: 21924436]
20. Shudo Y, Taniguchi K, Takeda K, Sakaguchi T, Funatsu T, Kondoh H, et al. Serial multidetector computed tomography assessment of left ventricular reverse remodeling, mass, and reginal wall stress after restrictive mitral annuloplasty in dilated cardiomyopathy. *J Thorac Cardiovasc Surg*. 2012; 143(4 Suppl):S43–47. [PubMed: 22169453]

PERSPECTIVE STATEMENT

Endogenous effectors of myocardial repair are likely not limited to a single cell type. Tissue engineered cell sheets offer the potential to exploit natural interactions between various cell types. Here, we demonstrate that co-administration of endothelial progenitor cells and smooth muscle cells as an intact construct significantly improves endogenous mechanisms of myocardial repair, and these cells are obtainable from a translationally relevant source.

CENTRAL MESSAGE

An EPC-SMC construct – derived entirely from bone marrow cells – augments neovascularization and attenuates post infarction myocardial remodeling.

Author Manuscript

Author Manuscript

Author Manuscript

Author Manuscript

CENTRAL PICTURE

EPC-SMC cell sheets enhance neovascularization and post infarction ventricular function.

Author Manuscript

Author Manuscript

Author Manuscript

Author Manuscript

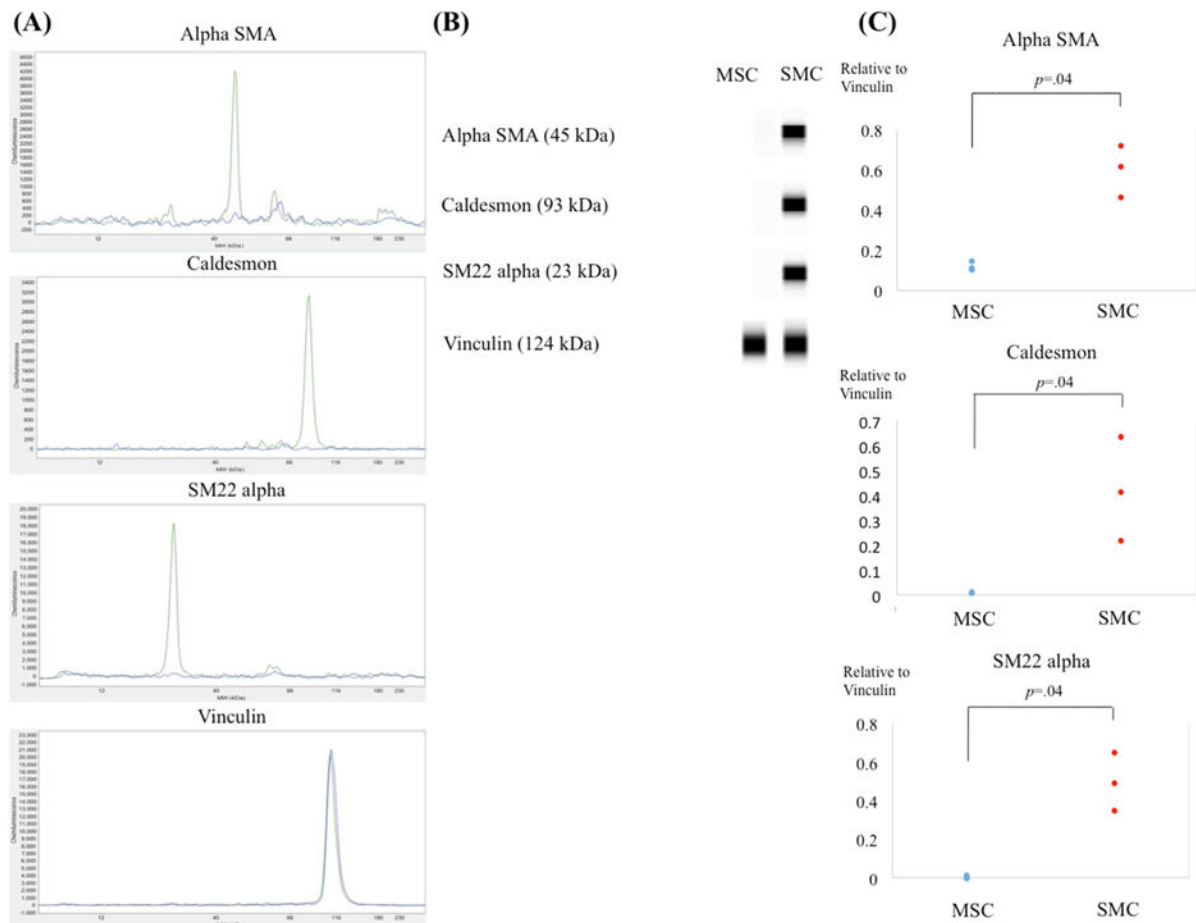


Figure 1.

Nanovolume capillary electrophoresis-based protein analysis was performed on cultured mesenchymal stem cells (MSCs) and transdifferentiated smooth muscle cells (SMCs) (MSC, $n=3$; SMC, $n=3$). **(A)** Electropherogram and system software generated peak area and molecular weight data linear analysis for alpha smooth muscle actin (SMA), SM22 alpha, and caldesmon between MSCs and SMCs. Green indicates SMC; blue, MSC. **(B)** Representative immunoblots for alpha SMA, SM22 alpha, and caldesmon between MSC and SMC. **(C)** Transdifferentiated SMCs demonstrated higher protein concentrations of alpha SMA, SM22 alpha, and caldesmon than MSCs. The intensity level of detected protein bands was standardized by dividing by the intensity level of vinculin.

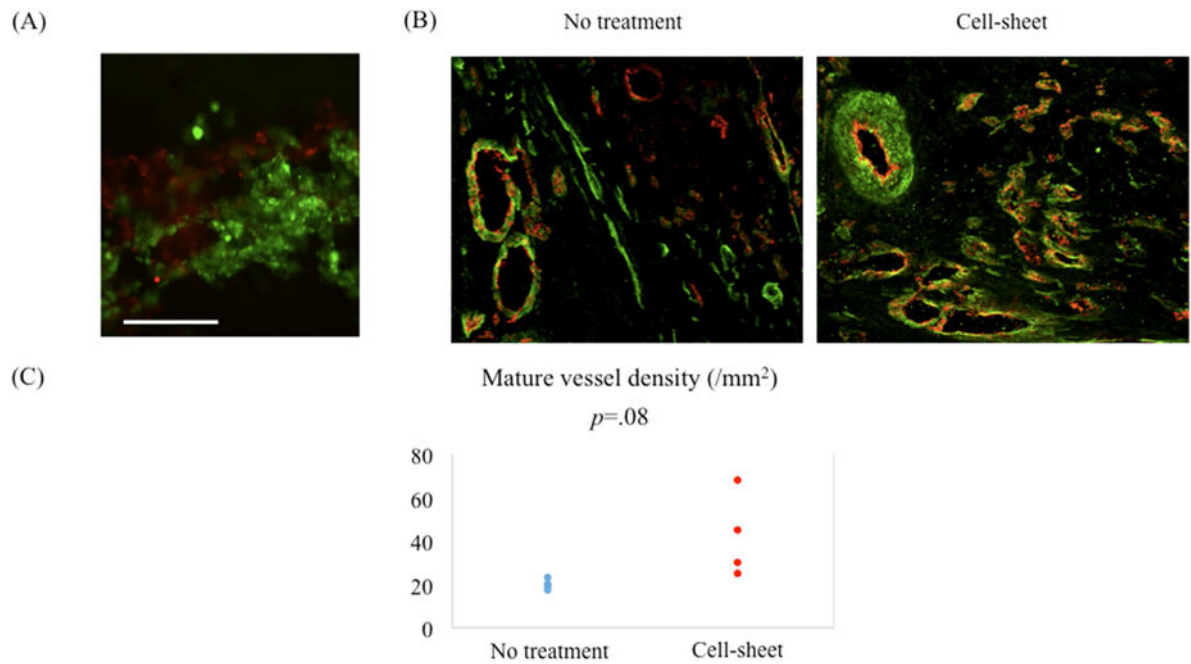


Figure 2.

(A) The bi-level cell sheet maintained alpha smooth muscle actin (SMA) positive smooth muscle cells (SMCs) and CD31 positive endothelial progenitor cells (EPCs) in separate layers in vitro. Green indicates alpha SMA; red, CD31. White bar = 100 μ m. (B) Representative images demonstrating von Willebrand factor (vWF) and alpha smooth muscle actin (SMA) staining of border zone myocardium for cell sheet-treated and untreated groups. Green indicates alpha SMA; red, vWF. (C) Quantification of arterial density. Mature artery density was increased in the cell sheet-treated group compared with the untreated group.

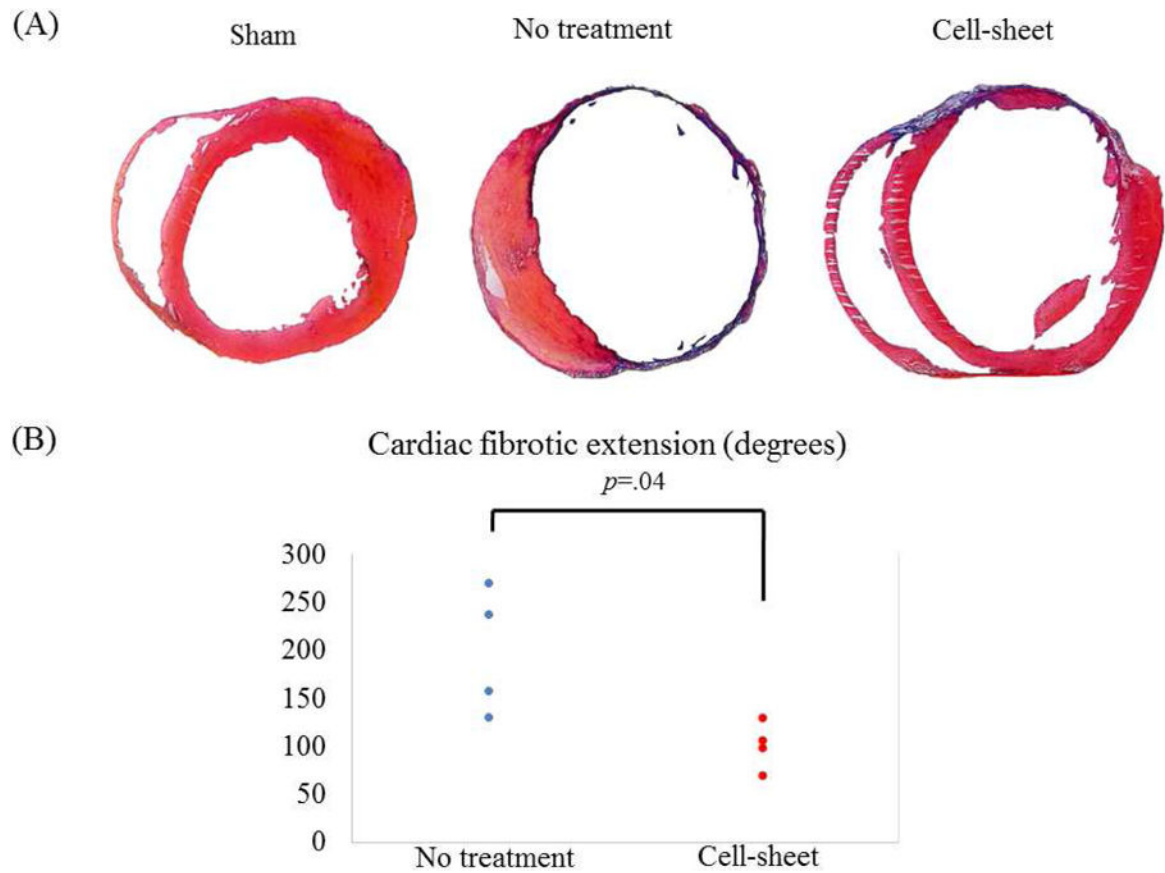


Figure 3.

(A) Representative Masson's trichrome staining of the heart for cell sheet-treated (n=4), untreated (n=4), and sham control (n=4) groups. (B) Quantification of cardiac fibrotic extension. Fibrosis was significantly suppressed in the cell-sheet group compared with the untreated group.

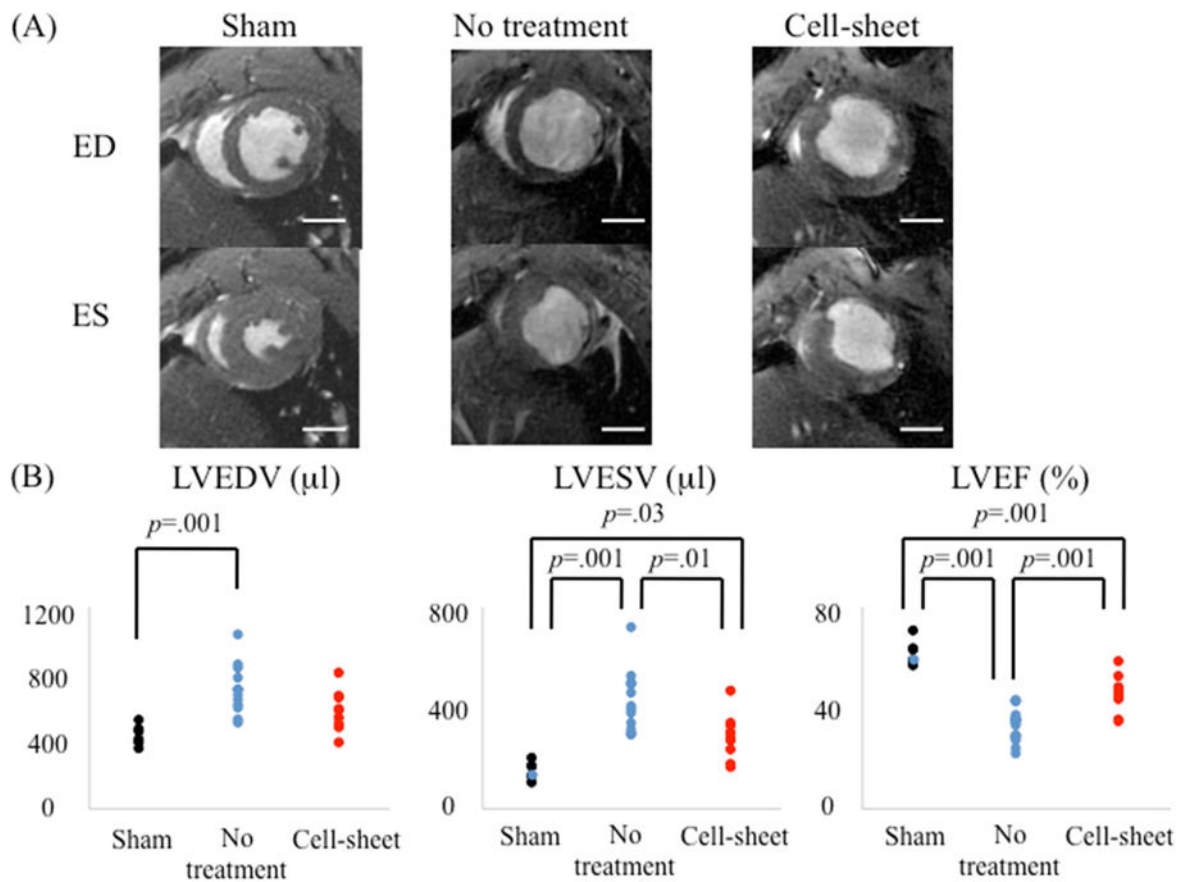


Figure 4.

(A) Representative cardiac magnetic resonance images at end-diastolic (ED) and end-systolic (ES) phases for cell sheet-treated (n=9), untreated (n=12), and sham control (n=7) groups. Examinations were performed 4 weeks after myocardial infarction. (B) Remarkable differences were noted between the three groups with respect to left ventricular end-diastolic volume (LVEDV), left ventricular end-systolic volume (LVESV), and ejection fraction (LVEF).